

# Text2VDM: Text to Vector Displacement Maps for Expressive and Interactive 3D Sculpting

Hengyu Meng<sup>1</sup> Duotun Wang<sup>1</sup> Zhijing Shao<sup>1</sup>  
Ligang Liu<sup>2</sup> Zeyu Wang<sup>1,3</sup>

<sup>1</sup>The Hong Kong University of Science and Technology (Guangzhou)

<sup>2</sup>University of Science and Technology of China

<sup>3</sup>The Hong Kong University of Science and Technology

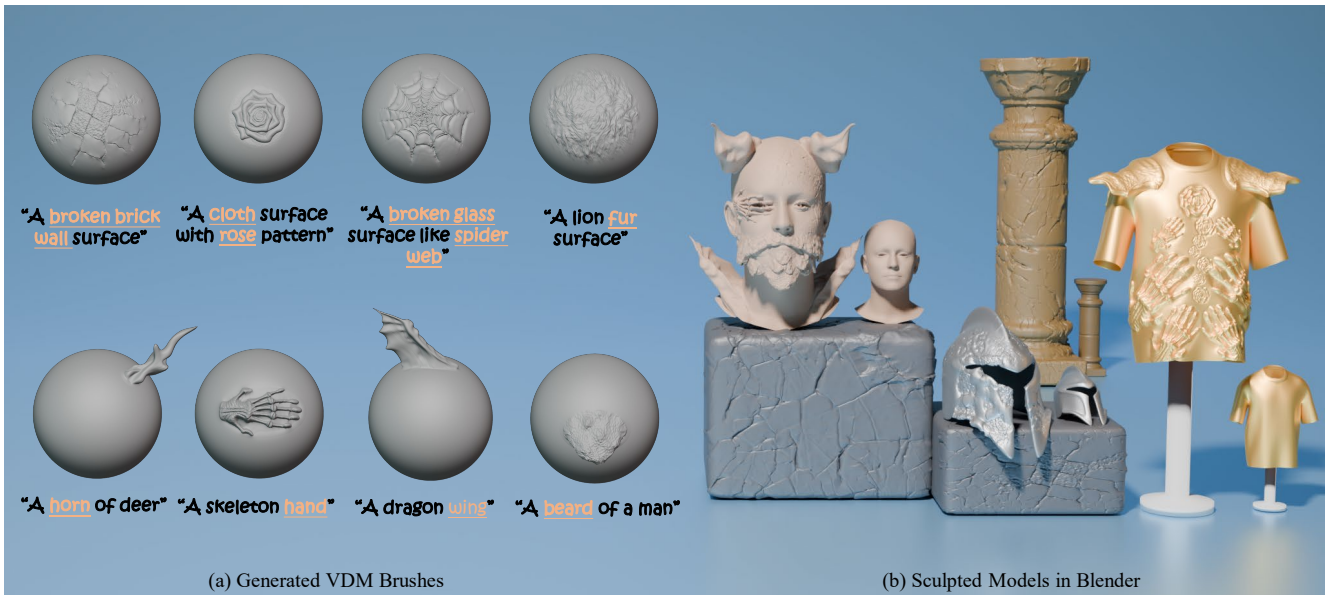


Figure 1. **Example VDM brushes generated by Text2VDM and sculpted models in Blender.** Text2VDM can produce high-quality brushes for surface details (top row) and geometric structures (bottom row) from text input. Users can rapidly create an expressive model from a plain shape by directly applying these brushes in Blender. Yellow underlined text highlights semantics enhanced by our framework.

## Abstract

Professional 3D asset creation often requires diverse sculpting brushes to add surface details and geometric structures. Despite recent progress in 3D generation, producing reusable sculpting brushes compatible with artists’ workflows remains an open and challenging problem. These sculpting brushes are typically represented as vector displacement maps (VDMs), which existing models cannot easily generate compared to natural images. This paper presents Text2VDM, a novel framework for text-to-VDM brush generation through the deformation of a dense planar mesh guided by score distillation sampling (SDS). The original SDS loss is designed for generating full objects

and struggles with generating desirable sub-object structures from scratch in brush generation. We refer to this issue as semantic coupling, which we address by introducing classifier-free guidance (CFG) weighted blending of prompt tokens to SDS, resulting in a more accurate target distribution and semantic guidance. Experiments demonstrate that Text2VDM can generate diverse, high-quality VDM brushes for sculpting surface details and geometric structures. Our generated brushes can be seamlessly integrated into mainstream modeling software, enabling various applications such as mesh stylization and real-time interactive modeling.

## 1. Introduction

Sculpting brushes are essential tools in 3D asset creation, as artists often require a variety of brushes to create surface details and geometric structures. In modeling software, 3D sculpting brushes are typically defined as vector displacement maps (VDMs). A VDM is a 2D image where each pixel stores a 3D displacement vector. Through these vectors, VDM brushes can create complex surface details, such as cracks and wood grain, or generate geometric structures like ears and horns. This allows artists to apply the same geometric pattern iteratively while sculpting.

Despite significant advances in text-to-image (T2I) [33, 40] and text-to-3D generation [20, 27, 34, 48, 49], existing methods are unsuitable for creating VDM brushes. We summarize the challenges as follows: 1) Since VDMs are not natural images (Figure 2), it is difficult for existing T2I models to generate them directly. 2) From a 3D perspective, a VDM represents mesh deformation through per-vertex displacement vectors from a dense planar mesh. Mapping any generated mesh to a dense planar mesh to create a VDM is non-trivial. 3) Sculpting brushes often involve sub-object structures, whereas most 3D generation methods can only generate full objects. Enabling users to accurately control the generation of sculpting brush through text descriptions in a semantically focused manner remains challenging.

To address the challenges of brush generation, we propose Text2VDM, a novel optimization-based framework that generates diverse and controllable VDM brushes from text input. Our approach does not generate VDMs directly from a T2I model. Instead, we address VDM brush generation from a 3D perspective by applying score distillation with a pre-trained T2I model to guide mesh deformation. Our framework supports three ways to initialize a base mesh through a zero-valued, spike-pattern, or user-specified VDM for custom shape control. We reparameterize the mesh vertices through an implicit formulation based on the Laplace-Beltrami operator [32] to achieve high-quality optimization of mesh deformations. We also provide optional region control using a mask of activated mesh deformation, helping users obtain the intended brush effects. We then rasterize normal maps of the mesh using a differentiable renderer for brush optimization.

We observed that the standard score distillation sampling (SDS) [34] can lead to semantic coupling when supervising the generation of sub-object level structures because of associated semantics noisy gradients of full object. For example, a generated tortoiseshell should not be a full tortoise with a head and a tail. A straightforward solution is to use negative prompts [17, 57] to exclude undesired semantics, but our experiments show that this approach is ineffective in decoupling semantics and leads to an unstable and more time-consuming optimization process. Instead, we propose to enhance the semantics of part-related words by applying

classifier-free guidance (CFG) weighted blending to the tokens in the prompt. This results in semantically focused text embedding, directing toward a more precise target distribution while reducing noisy gradients during optimization.

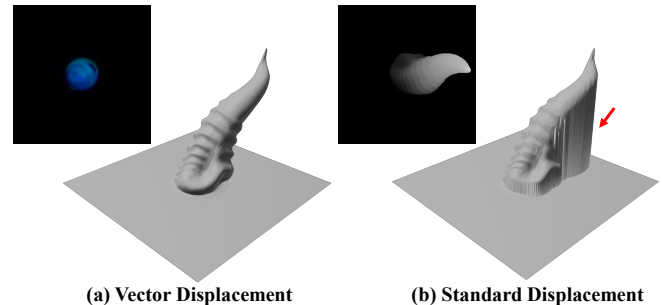


Figure 2. **Difference between vector and standard displacement.** The VDM enables full 3D vector displacement, while the height map only allows unidirectional standard displacement.

Our experiments demonstrate that Text2VDM produces high-quality and diverse VDM brushes that can be directly integrated into mainstream modeling software, such as Blender [5] and ZBrush [11]. Compared to existing methods that directly generate full 3D models, our approach addresses a different use case where brush-based user sculpting is desirable. We enable artists to interactively use a variety of brushes to sculpt diverse and expressive models from a plain shape.

This paper makes the following contributions:

- We first introduce the task of text-to-VDM brush generation, which is challenging to tackle directly using current text-to-image and text-to-3D methods.
- We propose Text2VDM, a novel framework for text-to-VDM brush generation that is readily compatible with artists’ workflow of 3D asset creation.
- We introduce CFG-weighted blending to SDS for modeling a more precise target distribution, mitigating semantic coupling in sub-object structure generation.

## 2. Related Work

This section reviews previous work related to 3D sculpting brush generation and summarizes the current research gap.

### 2.1. Text to Local 3D Generation and Editing

With recent advances in diffusion models [39] and differentiable 3D representations [1, 30, 32, 43, 45], many methods for text-guided full 3D model generation have emerged [7, 10, 20, 22, 28, 35, 41]. Since 3D content creation is an iterative process that often requires user interaction, more attention has been directed toward localized 3D generation and editing. For example, 3D Highlighter [8] and 3D Paintbrush [9] use text as input, leveraging pre-trained CLIP models [38] or diffusion models [34] to su-

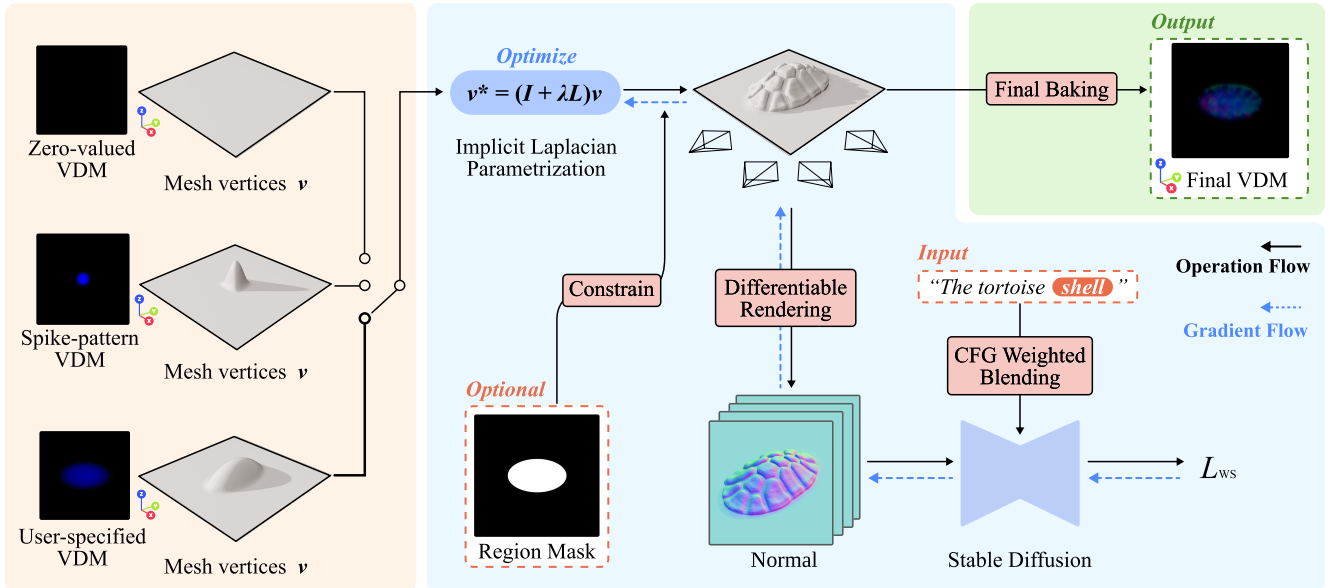


Figure 3. **Overview of Text2VDM.** Starting with a dense planar mesh constructed from a zero-valued VDM, users can initialize the mesh volume through a default spike-pattern VDM or a user-specified VDM. Given the text prompt and region mask, we apply CFG-weighted SDS loss  $\mathcal{L}_{ws}$  to guide mesh deformations through a Laplace-Beltrami operator  $L$  iteratively, achieving semantically focused generation of surface details or geometric structures. After optimization, vertex displacements are baked into the final VDM.

perverse the optimization of neural networks for segmenting the regions of a 3D model that match the text description. Based on the information from these segmented regions, further editing of texture and geometry can be applied to the 3D model. Furthermore, SKED [29] and SketchDream [24] introduce sketches as an additional modality to assist in localized editing. To enable more precise control, FocalDreamer [21], MagicClay [4], and Tip-Editor [58] allow users to specify the editing location directly within the 3D space. These works rely on optimization-based methods to edit specific objects, often resulting in non-reusable editing outcomes. Additionally, each edit requires a lengthy optimization process, making interactivity difficult to achieve.

## 2.2. Diffusion Priors for 3D Generation

Score distillation sampling (SDS) [34, 51] provides pixel-level guidance by seeking specific modes in a diffusion model, inspiring further research to improve optimization-based 3D generation [3, 23, 52, 53, 55]. Some studies focus on mitigating the “Janus” problem [2, 14], while others fine-tune diffusion models with multi-view datasets to enhance 3D consistency [25, 44]. Recent research focuses on refining the design of SDS loss to achieve more precise guidance. For instance, Make-it-3D [49] introduces two-stage optimizations to improve textured appearance, while Fantasia3D [7] dynamically modifies the time-dependent weighting function within SDS computations. Additionally, several methods [17, 57] incorporate negative prompts

as the conditional term to further refine the optimizations. Although diffusion priors have achieved promising results, their application in generating sub-object structures without global context as a reference is still challenging.

## 2.3. Appearance and Geometric Brush Synthesis

The concept of brushes is very common in the creative process of digital artists, serving as a reusable local decorative unit. Appearance brushes focus on color representation and drawing styles in 2D space. With the development of generative models [12, 39], many works have explored the synthesis appearance brushes for interactive painting [15, 46], realistic artworks generation [26, 31, 59], and applying stylization [16, 18]. Unlike appearance brushes, geometric brushes focus on modifying geometry by moving the vertices of a mesh in 3D space. VDM brushes, as an extension of standard geometric brushes, provide more complex geometric effects by utilizing VDMs. To the best of our knowledge, only a few techniques adopted the concepts of VDM for generation [42, 54] and geometric texture transfer [13]. Generating geometric brushes that can be used within existing workflows is still under-explored.

## 3. Methodology

Our framework can generate VDM brushes compatible with mainstream modeling software. As shown in Figure 3, we begin by constructing a dense mesh  $\mathcal{M}_0$  from an initial

VDM  $T_0$ . We then apply score distillation with a pretrained T2I diffusion model to guide mesh deformation through a Laplace-Beltrami operator  $L$  [32] toward the input text prompt  $y$ . The deformable region of the mesh can be controlled by an optional user-specified region mask  $R$ . To produce a high-quality sub-object level structure that only represents the intended part described by the text, we apply CFG-weighted blending to the tokens in the prompt, effectively handling the issue of semantic coupling in SDS.

### 3.1. Brush Initialization

We provide three methods to initialize a base mesh for brush generation via a zero-valued VDM, a spike-pattern VDM, or a user-specified VDM. A VDM is represented as a  $512 \times 512$  three-channel image, in which each channel stores the displacement in the X, Y, or Z direction respectively. We first construct a planar grid mesh by creating two triangles for every  $2 \times 2$  pixels and then apply the displacement stored in the VDM to mesh vertices. The values in these three initial VDMs range from 0 to 1, in which 0 represents no displacement, and 1 corresponds to half of the mesh’s edge length in the positive axis direction. Since users can apply sculpting brushes symmetrically, our initial VDM does not need to store any negative values.

Our three methods for brush initialization facilitate the generation of diverse sculpting brush styles. The zero-valued VDM results in a planar mesh, which is our default setup when no control is provided. The spike-pattern VDM is suitable for generating protruding geometric structures, as it can effectively adjust the Laplacian term in Equation (2) to steer the gradient direction for mesh deformation. For better control of the brush’s volume and direction, we also provide an interface for users to create custom VDMs, so the user-specified brush initialization can effectively guide mesh deformation toward the target structure.

### 3.2. Brush Generation via Mesh Deformation

Given the initialized based mesh, our method aims to learn a mesh deformation to the target brush shape. The vertex positions  $\hat{v}$  after mesh deformation can be expressed by

$$\hat{v} = \arg \min_v \mathcal{L}_{\text{WS}}(\mathcal{D}_c(v), y), \quad (1)$$

where  $c$  represents the camera setup in a differentiable renderer  $\mathcal{D}$  [19]. The loss function  $\mathcal{L}_{\text{WS}}$  receives the rendered normal image  $\mathcal{D}_c(v)$  and text input  $y$  to evaluate the semantic guidance, which is detailed in Section 3.3. In mesh deformation strategies, directly applying displacement to each vertex often results in unintended self-intersections of mesh faces caused by noisy gradients from pixel-level losses [28]. To address it, several works [10, 50] adopt the strategy by Aigerman et al. [1], parameterizing deformation by Jacobian fields that capture the scaling and rotation of each mesh

face. Although this method effectively smooths vertex displacements, the local deformation represented in Jacobians accumulates, leading to global drifting for open-boundary meshes, making it challenging to bake the mesh as a brush.

Based on these observations, we reparameterize the vertex optimization in Equation (1) through an implicit formulation with a Laplace-Beltrami operator  $L$ , similar to the approaches presented by Nicolet et al. [32]:

$$v^* = (I + \lambda L)v, \quad (2)$$

where  $I$  is the identity matrix,  $\lambda$  is a hyperparameter to control the extent of gradient diffusion from a given vertex to its neighboring vertices. When  $\lambda = 0$ , this representation degrades to direct vertex displacements. As  $\lambda$  increases, the mesh deforms toward more global structural changes. In our experiments, we set  $\lambda = 15$  to balance the global structure and fine details during mesh deformation (Figure 4). Additionally, we provide a region mask to restrict mesh deformation to the user-defined region during optimization. By adjusting the activation ratio of the region mask, the final brush effect can effectively match the user’s guidance. For instance, our experiment activated the region mask for the first half of total iterations as a warm-up stage to effectively control the shape of the surface detail (Figure 8). This differentiable parameterization effectively alters the gradient propagation at each optimization step as:

$$v^* \leftarrow v^* - \eta(I - \lambda L)^{-1} \frac{\partial \mathcal{L}_{\text{WS}}}{\partial v^*} \quad (3)$$

where  $\eta$  is the learning rate. The advantage of this Laplacian energy-aware mesh deformation is that it enhances the robustness of optimization for non-convex objective functions. The resulting mesh preserves the original structure while incorporating rich local deformations, making it well-suited for baking as a brush.

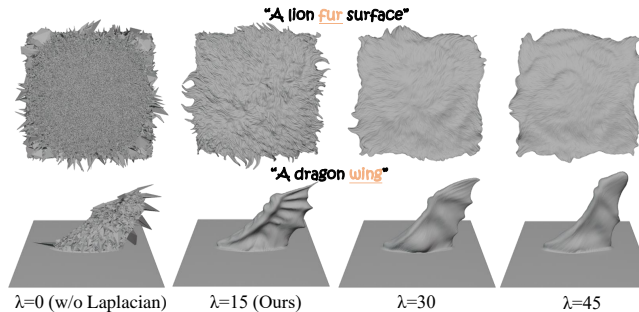


Figure 4. **Effects of  $\lambda$ .** As  $\lambda$  decreases, the mesh deformation shifts from global structural to locality, resulting in finer details, until it becomes a noisy surface at  $\lambda = 0$ .

### 3.3. CFG-Weighted Score Distillation Sampling

Current text-to-3D generation methods like DreamFusion [34] often optimize a 3D representation parameterized

by  $\theta$  so that rendered images  $\mathbf{x} = g(\theta)$  resemble 2D samples produced by a pre-trained T2I diffusion model for a given text prompt  $y$ .  $g$  functions as a differentiable renderer. The T2I diffusion model  $\phi$  predicts the sampled noise  $\epsilon_\phi(\mathbf{x}_t; y, t)$  of a rendered image  $\mathbf{x}_t$  at a noise level  $t$  for the text input  $y$ . To move all rendered images with higher density regions under the text-conditioned diffusion prior, SDS loss estimates the gradient for updating  $\theta$  as:

$$\nabla_\theta \mathcal{L}_{\text{SDS}}(\phi, \mathbf{x}) = \mathbb{E}_{t, \epsilon, c} \left[ \omega(t) (\epsilon_\phi(\mathbf{x}_t; y, t) - \epsilon) \frac{\partial \mathbf{x}}{\partial \theta} \right], \quad (4)$$

where  $\omega(t)$  is a time-dependent weighting function.

However, directly supervising sub-object structures with SDS, can lead to semantic coupling, which results in the generation of extra semantically related parts. For example, when generating a tortoiseshell, this semantic coupling will cause the generation of the tortoise’s tail and head (Figure 7). We believe that the issue of semantic coupling in SDS stems from the training data of the stable diffusion model, where images often depict partial components along with the complete object. This causes the target distribution conditioned by the text description of sub-object structures containing semantic information related to the full object.

A straightforward approach is using negative prompts proposed by classifier score distillation (CSD) [57] to mitigate coupled semantics. CSD demonstrates that compared to variational score distillation (VSD) [53], which adaptively learns negative classifier scores, CSD employs pre-defined negative prompts, resulting in a more precise optimization process:

$$\nabla_\theta \mathcal{L}_{\text{CSD}}(\phi, \mathbf{x}) = \mathbb{E}_{t, \epsilon, c} \left[ (\omega_1 \cdot \epsilon_\phi(\mathbf{x}_t; y, t) - \omega_2 \cdot \epsilon_\phi(\mathbf{x}_t; y_{\text{neg}}, t)) \frac{\partial \mathbf{x}}{\partial \theta} \right], \quad (5)$$

where  $\omega_1$  and  $\omega_2$  denote different weights for positive and negative prompts. We found that the negative prompt’s semantic distribution does not align with the associated semantics in the target distribution conditioned by the positive prompt of sub-object structures. This resulted in noisier gradients, making CSD less effective at decoupling semantics. Furthermore, as the weight of the negative prompt increased, the optimization became more unstable and challenging to converge.

Unlike CSD, we apply CFG-weighted blending to the tokens in the original prompt, which does not require additional inference to construct a negative distribution. This results in semantically focused text embedding, directing toward a more precise target distribution. Specifically, our loss function is defined as:

$$\nabla_\theta \mathcal{L}_{\text{WS}}(\phi, \mathbf{x}) = \mathbb{E}_{t, \epsilon, c} \left[ \omega(t) (\epsilon_\phi(\mathbf{x}_t; y^*, t) - \epsilon) \frac{\partial \mathbf{x}}{\partial \theta} \right], \quad (6)$$

where  $y^*$  is a text embedding computed by Compel [47]. Specifically, we assign each word in the prompt a CFG

weight  $s$  and compute the weighted embedding  $e_w$  for each word by blending the original text embedding  $e$  with the empty text embedding  $e_\phi$  as follows:  $e_w = e_\phi + s \cdot (e - e_\phi)$ . By concatenating the weighted embeddings of each word in sequence, we obtain the final semantically focused text embedding  $y^*$ . In our experiments, we found that assigning a weight of 1.21 to words that require enhanced semantics can achieve stable optimizations and effectively alleviate the issue of semantic coupling. Notably, the CFG weights used for text embedding computation are separate from the CFG guidance scale applied during the computation of the SDS loss. Our experiment uses a CFG guidance scale of 100.

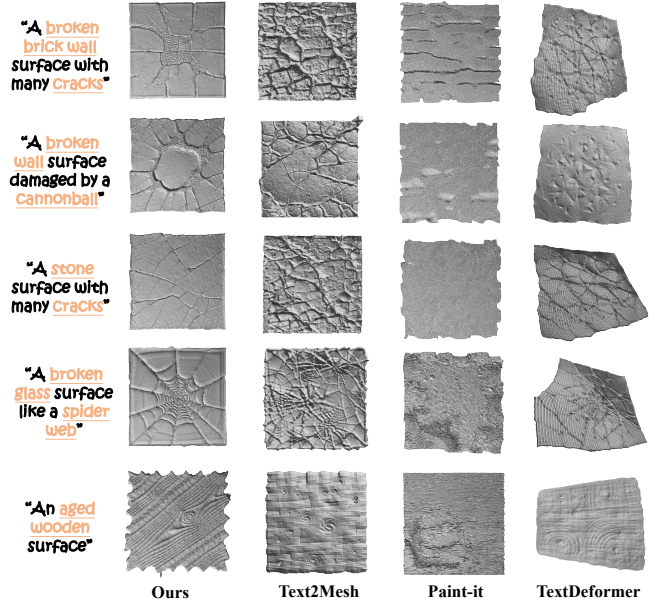


Figure 5. **Qualitative comparisons of generated brushes for surface details.** Our method captures geometry details guided by texts, effectively preserving surface structure and avoiding mesh distortions.

## 4. Experiments

In this section, we conduct experiments to evaluate the various capabilities of Text2VDM both quantitatively and qualitatively for text-to-VDM brush generation. We then present an ablation study that validates the significance of our key insight into CFG-weighted SDS, as well as the effect of the region control and shape control.

### 4.1. Qualitative Evaluation

To the best of our knowledge, Text2VDM is the first framework to generate VDM brushes from text. We adapted three existing methods for comparison and classified them into two categories. The first category includes Text2Mesh [28] and TextDeformer [10], which generate a brush mesh through text-guided mesh deformation on a planar mesh, following a process similar to ours. For the second cate-

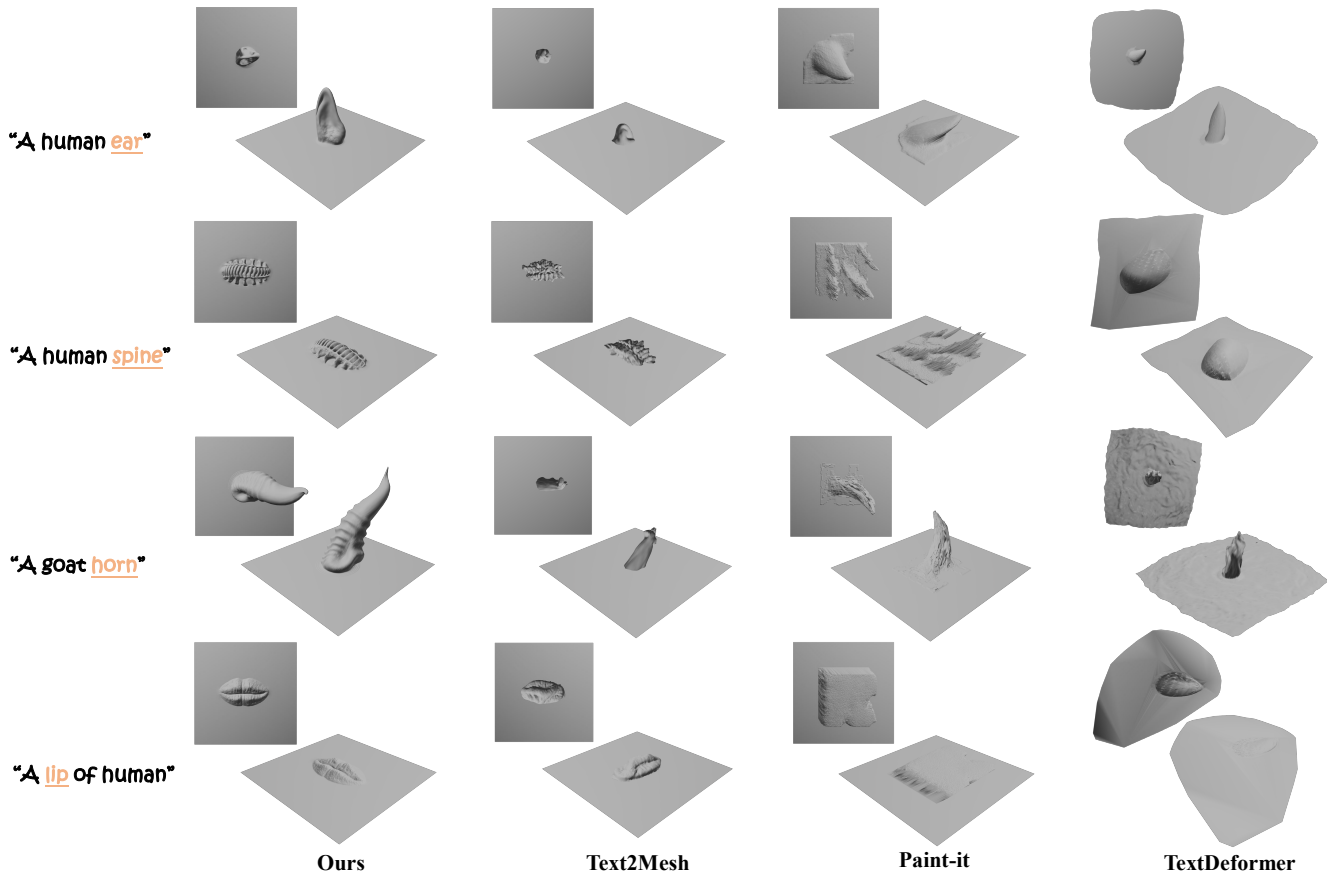


Figure 6. **Qualitative comparisons of generated brushes for geometric structures.** Our method accurately presents key geometric features described by text, facilitating downstream applications in modeling software.

gory, we opt to directly generate VDM via Paint-it [56]. Notably, this method originally uses SDS to optimize a UNet for generating PBR textures. We reframed it to suit our VDM brush generation task, modifying it to generate VDM through SDS optimization of the UNet. We compared the visual results in Figure 5 and Figure 6.

Compared to other methods, Text2VDM can generate more vivid and better-quality VDM brushes. Text2Mesh applies displacement to each vertex along normal directions, resulting in limited mesh deformation. TextDeformer indicates the accumulation of local deformations in the Jacobians, which results in global mesh drift, making it challenging to bake these meshes into VDM. Reframed Paint-it VDM generation is equivalent to optimizing the three-axis displacement of each vertex on the mesh with SDS. Although the UNet reduces noise from the SDS [56], geometric regularization is still required to ensure mesh quality. The generated mesh must compromise between solving the problem and maintaining smoothness, which makes achieving high-quality mesh generation quite challenging.

## 4.2. Quantitative Evaluation

We quantitatively evaluated our framework regarding generation consistency with text input and mesh quality. We used 40 distinctive text prompts for VDM generation.

**Generation Consistency with Text.** We initially assessed the relevance of the generated results to the text descriptions [37]. 12 different views were rendered for average scores respectively, as presented in Table 1. Our approach achieves the highest scores compared to baseline methods.

Table 1. Quantitative evaluation of state-of-the-art methods. The geometry CLIP score is calculated on shaded images with uniform albedo colors [36], and self-intersection is quantified as the ratio of self-intersected mesh faces to the total number of faces.

	Geometry CLIP Score $\uparrow$	Mesh Self-Intersection $\downarrow$
Paintit	0.2375	19.42%
Text2Mesh	0.2497	7.18%
TextDeformer	0.2477	<b>0.04%</b>
Ours	<b>0.2556</b>	0.77%

**Mesh Quality.** We evaluated mesh quality by examining self-intersection. Paint-it and Text2Mesh, which utilize di-

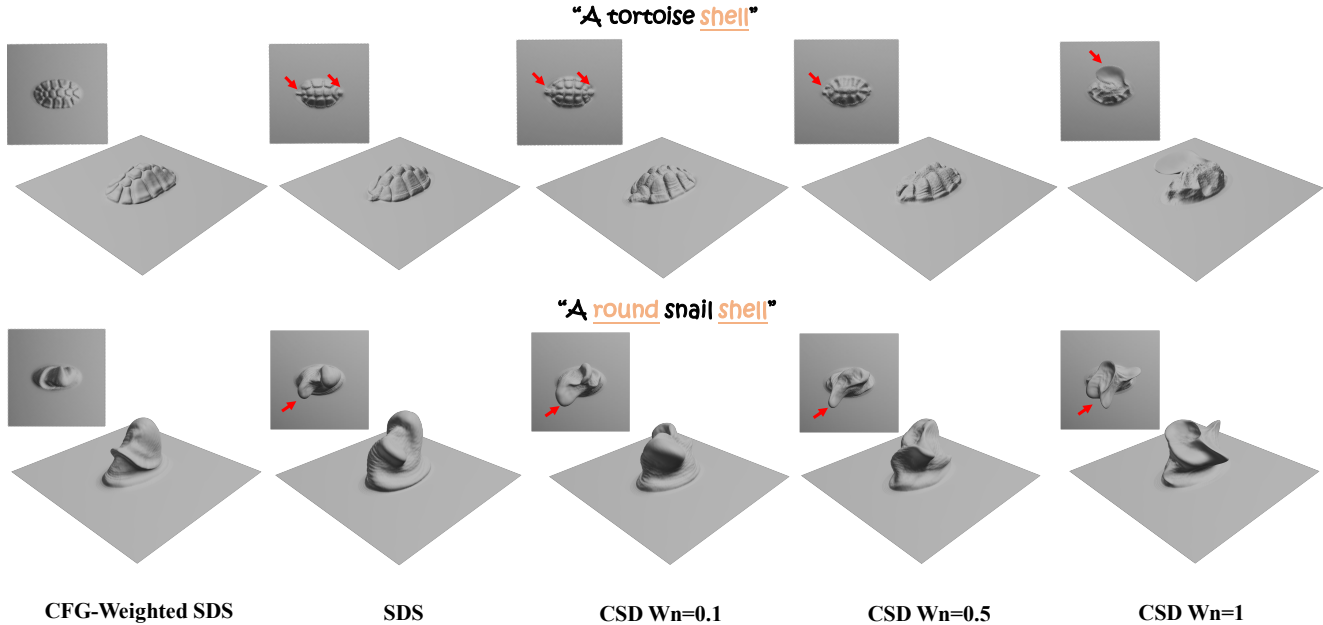


Figure 7. **Effect of CFG-weighted SDS.** CFG-weighted SDS effectively mitigates semantic coupling issues in SDS, such as generating the tortoise’s tail and head or the snail’s head, by providing more focused semantic guidance. In contrast, CSD adds extra negative terms that fail to decouple semantics, resulting in a less stable and more time-consuming optimization process.

rect vertex displacement, often converge to a local minimum and disregard the mesh triangulation. While TextDeformer exhibits the lowest self-intersection, its tendency to produce over-smoothed results frequently results in losing object features described in text prompts.

Table 2. User evaluation of generated VDMs.

User Preference $\uparrow$	Geometry Quality	Consistency with Text
Paintit	3.1%	1.7%
Text2Mesh	18.3%	27.3%
TextDeformer	3.3%	3.4%
Ours	<b>75.3%</b>	<b>67.6%</b>

**User Study.** We further conducted a user study to evaluate the effectiveness and expressiveness of our method. A Google Form was utilized to assess 1) geometry quality and 2) consistency with text. We recruited 32 participants, of whom 14 are graduate students majoring in media arts, and 18 are company employees specializing in AI content generation. In this form, the participants were instructed to choose the preferred renderings of VDM from different methods in randomized order, as shown in Table 2. The results show participants preferred our method by a significant margin.

### 4.3. Ablation Study

**Effects of CFG-Weighted SDS.** We conducted experiments to compare the generated results of directly using SDS [34], CFG-weighted SDS, and CSD [57] with three

different annealed weights of negative prompt (Figure 7). As discussed in Section 3.3, SDS can result in semantic coupling when generating sub-object structure, leading to artifacts like the tortoise’s tail and head or the snail’s head. We also found that using negative prompts was ineffective at decoupling semantics. Increasing the initial weight of negative prompts further makes the optimization unstable, resulting in low-quality results. In contrast, our method effectively mitigates semantic coupling to produce high-quality meshes without requiring additional UNet inference.

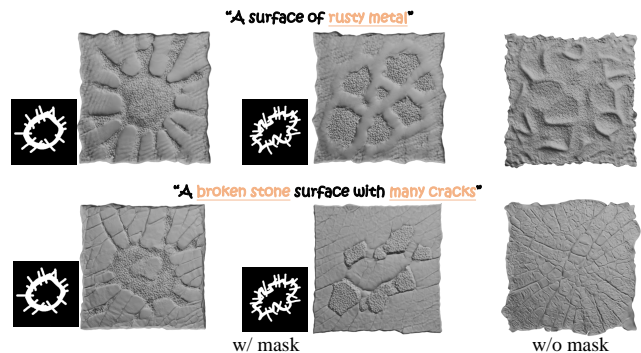


Figure 8. **Effect of region control.** Region masks can effectively control the shape of surface details based on different text inputs.

**Effects of Region Control.** Figure 8 demonstrates two sets of region masks and their control over surface details generation under different text prompts. Without using a region

mask, the results lack a specific shape, which may not satisfy the desired stylized effect. By using a region mask, our generated results effectively conform to the user’s desired shapes while also aligning with the styles specified by the text, such as metal and stone.

**Effects of Shape Control.** Our method demonstrates that user-specified VDMs can effectively control the volume and direction of generated geometric structures. As shown in Figure 9, various generated geometric structures, such as elf ears and pauldrons, are high-quality and align with the text descriptions. We also found that without volume initialization, it is challenging to generate desired results. It indicates that this initialization is crucial for steering the gradient flow of geometric structure generation via adjusting the Laplacian term.

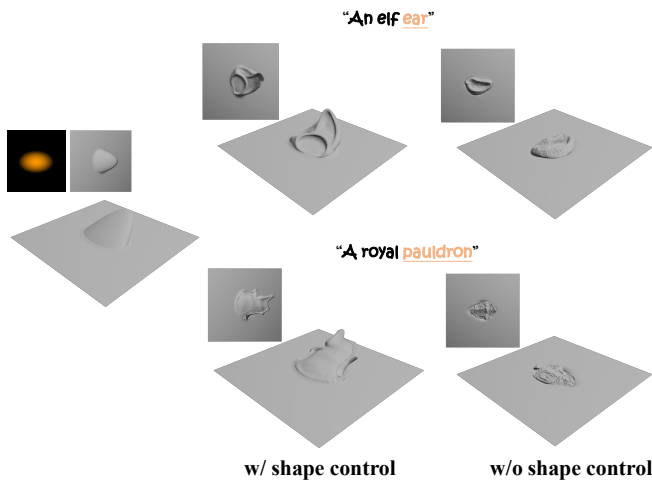


Figure 9. **Effect of shape control.** User-specified VDMs can help achieve the intended final effect of geometric structures by initializing the brush’s volume and direction.

#### 4.4. Applications

Once various VDM brushes are generated, users can directly use these brushes to meet diverse creative needs in mainstream modeling software. For example, they can apply VDM brushes for mesh stylization and engage in a real-time iterative modeling process.

**Local-to-Global Mesh Stylization.** Although mesh stylization is a complex task even for professional artists, combining different surface details allows users to achieve stylization quickly. For instance, users can apply a variety of wall-damage brushes to specific areas of a stone pillar, creating a style of damage (Figure 10).

**Coarse-to-Fine Interactive Modeling.** Unlike previous methods [4, 58] that require a lengthy optimization process for each edit and result in non-reusable outcomes, our generated VDM brushes can be directly used in modeling software. This enables users to apply the generated brushes easily and interactively. For example, Figure 11 shows that

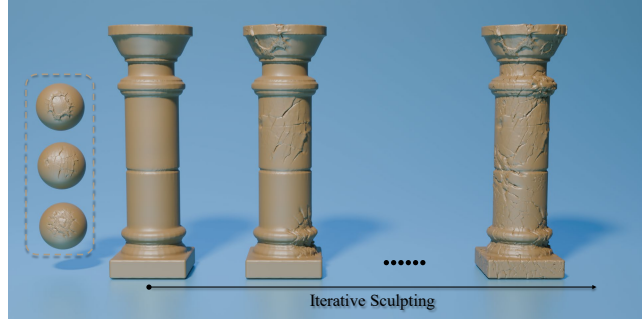


Figure 10. **Local to global mesh stylization.** Applying various surface details brushes can create a damaged-style stone pillar model.



Figure 11. **Coarse to fine interactive modeling.** By combining geometric structures brushes and surface details brushes for iterative sculpting in modeling software, users can rapidly create an expressive model from a plain shape (top left).

users can combine various brushes, such as skeleton hand, rose pattern, and pauldron to refine a coarse cloth model into a highly detailed one.

#### 5. Conclusion

We have presented Text2VDM, a novel framework for VDM brush generation from text. A VDM is a non-natural 2D image where each pixel stores a 3D displacement vector, making it challenging for existing T2I models to generate. Thus, We treat VDM generation as mesh deformation via the Laplace-Beltrami operator from a dense planar mesh. To generate the intended effects of surface details and geometric structures, we provide two control methods: region control and shape control. Additionally, VDM brushes often contain sub-object structures, which can lead to semantic coupling issues in SDS. We propose using CFG-weighted blending for prompt tokens to effectively mitigate this, achieving high-quality brush generation. The generated VDM brushes are directly compatible with mainstream modeling software, enabling various applications such as mesh stylization and real-time interactive modeling.

**Limitations and future work.** While our framework



can generate high-quality VDM brushes, they may encounter multi-view inconsistencies, a common issue introduced by SDS. To further address it, the view-consistent diffusion model proposed in MV2MV [6] may be helpful.

## References

- [1] Noam Aigerman, Kunal Gupta, Vladimir G. Kim, Siddhartha Chaudhuri, Jun Saito, and Thibault Groueix. Neural Jacobian Fields: Learning Intrinsic Mappings of Arbitrary Meshes. *ACM Trans. Graph.*, 41(4), 2022. 2, 4
- [2] Thimo Alldieck, Nikos Kolotouros, and Cristian Sminchisescu. Score Distillation Sampling with Learned Manifold Corrective. *arXiv preprint 2401.05293*, 2024. 3
- [3] Mohammadreza Armandpour, Ali Sadeghian, Huangjie Zheng, Amir Sadeghian, and Mingyuan Zhou. Re-imagine the Negative Prompt Algorithm: Transform 2D Diffusion into 3D, alleviate Janus problem and Beyond. *arXiv preprint 2304.04968*, 2023. 3
- [4] Amir Barda, Vladimir G. Kim, Noam Aigerman, Amit H. Bermano, and Thibault Groueix. MagicClay: Sculpting Meshes with Generative Neural Fields. *SIGGRAPH Asia (Conference track)*, 2024. 3, 8
- [5] community Blender Foundation. Blender. <https://www.blender.org>, 1994. Accessed Oct 22, 2024. 2
- [6] Youcheng Cai, Runshi Li, and Ligang Liu. MV2MV: Multi-View Image Translation via View-Consistent Diffusion Models. *ACM Trans. Graph.*, 2024. 9
- [7] Rui Chen, Yongwei Chen, Ningxin Jiao, and Kui Jia. Fantasia3D: Disentangling Geometry and Appearance for High-quality Text-to-3D Content Creation. In *Proceedings of the IEEE/CVF International Conference on Computer Vision*, pages 22246–22256, 2023. 2, 3
- [8] Dale Decatur, Itai Lang, and Rana Hanocka. 3D Highlighter: Localizing Regions on 3D Shapes via Text Descriptions. In *Proceedings of the IEEE/CVF Conference on Computer Vision and Pattern Recognition*, pages 20930–20939, 2023. 2
- [9] Dale Decatur, Itai Lang, Kfir Aberman, and Rana Hanocka. 3D Paintbrush: Local Stylization of 3D Shapes with Cascaded Score Distillation. In *Proceedings of the IEEE/CVF Conference on Computer Vision and Pattern Recognition (CVPR)*, pages 4473–4483, 2024. 2
- [10] William Gao, Noam Aigerman, Thibault Groueix, Vova Kim, and Rana Hanocka. TextDeformer: Geometry Manipulation Using Text Guidance. In *ACM SIGGRAPH 2023 Conference Proceedings*, New York, NY, USA, 2023. Association for Computing Machinery. 2, 4, 5
- [11] Maxon Computer GMBH. ZBrush. <https://www.maxon.net/zbrush>, 1999. Accessed Oct 18, 2024. 2
- [12] Ian Goodfellow, Jean Pouget-Abadie, Mehdi Mirza, Bing Xu, David Warde-Farley, Sherjil Ozair, Aaron Courville, and Yoshua Bengio. Generative Adversarial Nets. *Advances in Neural Information Processing Systems*, 27, 2014. 3
- [13] Amir Hertz, Rana Hanocka, Raja Giryes, and Daniel Cohen-Or. Deep Geometric Texture Synthesis. *ACM Trans. Graph.*, 39(4), 2020. 3
- [14] Susung Hong, Donghoon Ahn, and Seungryong Kim. De-biasing Scores and Prompts of 2D Diffusion for View-consistent Text-to-3D Generation. In *Neural Information Processing Systems*, 2023. 3
- [15] Anita Hu, Nishkrit Desai, Hassan Abu Alhajja, Seung Wook Kim, and Maria Shugrina. Diffusion Texture Painting. New York, NY, USA, 2024. Association for Computing Machinery. 3
- [16] Teng Hu, Ran Yi, Haokun Zhu, Liang Liu, Jinlong Peng, Yabiao Wang, Chengjie Wang, and Lizhuang Ma. Stroke-based Neural Painting and Stylization with Dynamically Predicted Painting Region. New York, NY, USA, 2023. Association for Computing Machinery. 3
- [17] Oren Katzir, Or Patashnik, Daniel Cohen-Or, and Dani Lischinski. Noise-free Score Distillation. In *The Twelfth International Conference on Learning Representations*, 2024. 2, 3
- [18] Dmytro Kotovenko, Matthias Wright, Arthur Heimbrecht, and Björn Ommer. Rethinking Style Transfer: From Pixels to Parameterized Brushstrokes. *2021 IEEE/CVF Conference on Computer Vision and Pattern Recognition (CVPR)*, pages 12191–12200, 2021. 3
- [19] Samuli Laine, Janne Hellsten, Tero Karras, Yeongho Seol, Jaakko Lehtinen, and Timo Aila. Modular Primitives for High-Performance Differentiable Rendering. *ACM Transactions on Graphics*, 39(6), 2020. 4
- [20] Jiahao Li, Hao Tan, Kai Zhang, Zexiang Xu, Fujun Luan, Yinghao Xu, Yicong Hong, Kalyan Sunkavalli, Greg Shakhnarovich, and Sai Bi. Instant3D: Fast Text-to-3D with Sparse-View Generation and Large Reconstruction Model. *arXiv preprint 2311.06214*, 2023. 2
- [21] Yuhan Li, Yishun Dou, Yue Shi, Yu Lei, Xuanhong Chen, Yi Zhang, Peng Zhou, and Bingbing Ni. FocalDreamer: Text-Driven 3D Editing via Focal-Fusion Assembly. *Proceedings of the AAAI Conference on Artificial Intelligence*, 38:3279–3287, 2024. 3
- [22] Yixun Liang, Xin Yang, Jiantao Lin, Haodong Li, Xiaogang Xu, and Yingcong Chen. LucidDreamer: Towards High-Fidelity Text-to-3D Generation via Interval Score Matching. *2024 IEEE/CVF Conference on Computer Vision and Pattern Recognition (CVPR)*, pages 6517–6526, 2023. 2
- [23] Chen-Hsuan Lin, Jun Gao, Luming Tang, Towaki Takikawa, Xiaohui Zeng, Xun Huang, Karsten Kreis, Sanja Fidler, Ming-Yu Liu, and Tsung-Yi Lin. Magic3D: High-Resolution Text-to-3D Content Creation. In *Proceedings of the IEEE/CVF Conference on Computer Vision and Pattern Recognition*, pages 300–309, 2023. 3
- [24] Feng-Lin Liu, Hongbo Fu, Yu-Kun Lai, and Lin Gao. SketchDream: Sketch-based Text-to-3D Generation and Editing. *ACM Transactions on Graphics (Proceedings of ACM SIGGRAPH 2024)*, 43(4), 2024. 3
- [25] Ruoshi Liu, Rundi Wu, Basile Van Hoorick, Pavel Tokmakov, Sergey Zakharov, and Carl Vondrick. Zero-1-to-3: Zero-shot One Image to 3D Object. *Proceedings of the IEEE/CVF International Conference on Computer Vision*, pages 9264–9275, 2023. 3
- [26] Songhua Liu, Tianwei Lin, Dongliang He, Fu Li, Ruifeng Deng, Xin Li, Errui Ding, and Hao Wang. Paint Transformer:

- Feed Forward Neural Painting with Stroke Prediction. In *Proceedings of the IEEE/CVF International Conference on Computer Vision*, pages 6578–6587, 2021. 3
- [27] Xiaoxiao Long, Yuanchen Guo, Cheng Lin, Yuan Liu, Zhiyang Dou, Lingjie Liu, Yuexin Ma, Song-Hai Zhang, Marc Habermann, Christian Theobalt, and Wenping Wang. Wonder3D: Single Image to 3D Using Cross-Domain Diffusion. *2024 IEEE/CVF Conference on Computer Vision and Pattern Recognition (CVPR)*, pages 9970–9980, 2023. 2
- [28] Oscar Michel, Roi Bar-On, Richard Liu, Sagie Benaim, and Rana Hanocka. Text2Mesh: Text-Driven Neural Stylization for Meshes. In *2022 IEEE/CVF Conference on Computer Vision and Pattern Recognition (CVPR)*, pages 13482–13492, 2022. 2, 4, 5
- [29] Aryan Mikaeili, Or Perel, Mehdi Safaei, Daniel Cohen-Or, and Ali Mahdavi-Amiri. SKED: Sketch-guided Text-based 3D Editing. *Proceedings of the IEEE/CVF International Conference on Computer Vision*, 2023. 3
- [30] Ben Mildenhall, Pratul P Srinivasan, Matthew Tancik, Jonathan T Barron, Ravi Ramamoorthi, and Ren Ng. NeRF: Representing Scenes as Neural Radiance Fields for View Synthesis. In *European Conference on Computer Vision*, pages 405–421, 2020. 2
- [31] Haoran Mo, Edgar Simo-Serra, Chengying Gao, Changqing Zou, and Ruomei Wang. General virtual sketching framework for vector line art. *ACM Transactions on Graphics (TOG)*, 40:1 – 14, 2021. 3
- [32] Baptiste Nicolet, Alec Jacobson, and Wenzel Jakob. Large Steps in Inverse Rendering of Geometry. *ACM Trans. Graph.*, 40(6), 2021. 2, 4
- [33] Openai. DALL-E. <https://openai.com/index/dall-e-3/>, 2024. Accessed Oct 22, 2024. 2
- [34] Ben Poole, Ajay Jain, Jonathan T Barron, and Ben Mildenhall. DreamFusion: Text-to-3D using 2D Diffusion. In *The Eleventh International Conference on Learning Representations*, 2022. 2, 3, 4, 7
- [35] Lingteng Qiu, Guanying Chen, Xiaodong Gu, Qi Zuo, Mutian Xu, Yushuang Wu, Weihao Yuan, Zilong Dong, Liefeng Bo, and Xiaoguang Han. RichDreamer: A Generalizable Normal-Depth Diffusion Model for Detail Richness in Text-to-3D. *2024 IEEE/CVF Conference on Computer Vision and Pattern Recognition (CVPR)*, pages 9914–9925, 2023. 2
- [36] Lingteng Qiu, Guanying Chen, Xiaodong Gu, Qi Zuo, Mutian Xu, Yushuang Wu, Weihao Yuan, Zilong Dong, Liefeng Bo, and Xiaoguang Han. RichDreamer: A Generalizable Normal-Depth Diffusion Model for Detail Richness in Text-to-3D. In *Proceedings of the IEEE/CVF Conference on Computer Vision and Pattern Recognition (CVPR)*, pages 9914–9925, 2024. 6
- [37] Alec Radford, Jong Wook Kim, Chris Hallacy, Aditya Ramesh, Gabriel Goh, Sandhini Agarwal, Girish Sastry, Amanda Askell, Pamela Mishkin, Jack Clark, Gretchen Krueger, and Ilya Sutskever. Learning Transferable Visual Models From Natural Language Supervision. *arXiv preprint arXiv:2103.00020*, 2021. 6
- [38] Alec Radford, Jong Wook Kim, Chris Hallacy, Aditya Ramesh, Gabriel Goh, Sandhini Agarwal, Girish Sastry, Amanda Askell, Pamela Mishkin, Jack Clark, Gretchen Krueger, and Ilya Sutskever. Learning Transferable Visual Models From Natural Language Supervision. In *International Conference on Machine Learning*, 2021. 2
- [39] Robin Rombach, Andreas Blattmann, Dominik Lorenz, Patrick Esser, and Björn Ommer. High-Resolution Image Synthesis With Latent Diffusion Models. In *Proceedings of the IEEE/CVF Conference on Computer Vision and Pattern Recognition (CVPR)*, pages 10684–10695, 2022. 2, 3
- [40] Robin Rombach, Andreas Blattmann, Dominik Lorenz, Patrick Esser, and Björn Ommer. High-resolution image synthesis with latent diffusion models. In *2022 IEEE/CVF Conference on Computer Vision and Pattern Recognition (CVPR)*, pages 10674–10685, 2022. 2
- [41] Aditya Sanghi, Hang Chu, Joseph G Lambourne, Ye Wang, Chin-Yi Cheng, Marco Fumero, and Kamal Rahimi Malekshah. Clip-forge: Towards Zero-shot Text-to-shape Generation. In *Proceedings of the IEEE/CVF Conference on Computer Vision and Pattern Recognition*, pages 18603–18613, 2022. 2
- [42] Artem Sevastopolsky, Philip-William Grassal, Simon Giebenhain, ShahRukh Athar, Luisa Verdoliva, and Matthias Niessner. Headcraft: Modeling high-detail shape variations for animated 3dmm, 2023. 3
- [43] Tianchang Shen, Jun Gao, Kangxue Yin, Ming-Yu Liu, and Sanja Fidler. Deep Marching Tetrahedra: a Hybrid Representation for High-resolution 3D Shape Synthesis. *Advances in Neural Information Processing Systems*, 34:6087–6101, 2021. 2
- [44] Yichun Shi, Peng Wang, Jianglong Ye, Long Mai, Kejie Li, and Xiao Yang. MVDream: Multi-view Diffusion for 3D Generation. In *The Twelfth International Conference on Learning Representations*, 2024. 3
- [45] J. Ryan Shue, Eric Ryan Chan, Ryan Po, Zachary Ankner, Jiajun Wu, and Gordon Wetzstein. 3D Neural Field Generation Using Triplane Diffusion. In *2023 IEEE/CVF Conference on Computer Vision and Pattern Recognition (CVPR)*, pages 20875–20886, 2023. 2
- [46] Maria Shugrina, Chin-Ying Li, and Sanja Fidler. Neural Brushstroke Engine: Learning a Latent Style Space of Interactive Drawing Tools. *ACM Trans. Graph.*, 41(6), 2022. 3
- [47] Damian Stewart. Compel: A Text Prompt Weighting and Blending Library. <https://github.com/damian0815/compel>, 2023. Accessed Oct 20, 2024. 5
- [48] Jiaxiang Tang, Jiawei Ren, Hang Zhou, Ziwei Liu, and Gang Zeng. DreamGaussian: Generative Gaussian Splatting for Efficient 3D Content Creation, 2023. 2
- [49] Junshu Tang, Tengfei Wang, Bo Zhang, Ting Zhang, Ran Yi, Lizhuang Ma, and Dong Chen. Make-It-3D: High-fidelity 3D Creation from A Single Image with Diffusion Prior. In *Proceedings of the IEEE/CVF International Conference on Computer Vision*, pages 22819–22829, 2023. 2, 3
- [50] Duotun Wang, Hengyu Meng, Zeyu Cai, Zhijing Shao, Qianxi Liu, Lin Wang, Mingming Fan, Xiaohang Zhan, and Zeyu Wang. HeadEvolver: Text to Head Avatars via Expressive and Attribute-Preserving Mesh Deformation. *arXiv preprint arXiv:2403.09326*, 2023. 4

- [51] Haochen Wang, Xiaodan Du, Jiahao Li, Raymond A Yeh, and Greg Shakhnarovich. Score Jacobian Chaining: Lifting Pretrained 2D Diffusion Models for 3D Generation. In *Proceedings of the IEEE/CVF Conference on Computer Vision and Pattern Recognition*, pages 12619–12629, 2023. [3](#)
- [52] Peihao Wang, Dejie Xu, Zhiwen Fan, Dilin Wang, Sreyas Mohan, Forrest N. Iandola, Rakesh Ranjan, Yilei Li, Qiang Liu, Zhangyang Wang, and Vikas Chandra. Taming Mode Collapse in Score Distillation for Text-to-3D Generation. *arXiv preprint 2401.00909*, 2023. [3](#)
- [53] Zhengyi Wang, Cheng Lu, Yikai Wang, Fan Bao, Chongxuan Li, Hang Su, and Jun Zhu. ProlificDreamer: High-fidelity and Diverse Text-to-3D Generation with Variational Score Distillation. In *Proceedings of the 37th International Conference on Neural Information Processing Systems*, Red Hook, NY, USA, 2024. Curran Associates Inc. [3](#), [5](#)
- [54] Xingguang Yan, Han-Hung Lee, Ziyu Wan, and Angel X. Chang. An Object is Worth 64x64 Pixels: Generating 3D Object via Image Diffusion, 2024. [3](#)
- [55] Xiaofeng Yang, Yiwen Chen, Cheng Chen, Chi Zhang, Yi Xu, Xulei Yang, Fayao Liu, and Guosheng Lin. Learn to Optimize Denoising Scores for 3D Generation: A Unified and Improved Diffusion Prior on NeRF and 3D Gaussian Splatting. *arXiv preprint 2312.04820*, 2023. [3](#)
- [56] Kim Youwang, Tae-Hyun Oh, and Gerard Pons-Moll. Paint-it: Text-to-Texture Synthesis via Deep Convolutional Texture Map Optimization and Physically-Based Rendering. In *IEEE Conference on Computer Vision and Pattern Recognition (CVPR)*, 2024. [6](#)
- [57] Xin Yu, Yuanchen Guo, Yangguang Li, Ding Liang, Song-Hai Zhang, and Xiaojuan Qi. Text-to-3D with Classifier Score Distillation. *arXiv preprint 2310.19415*, 2023. [2](#), [3](#), [5](#), [7](#)
- [58] Jingyu Zhuang, Di Kang, Yan-Pei Cao, Guanbin Li, Liang Lin, and Ying Shan. TIP-Editor: An Accurate 3D Editor Following Both Text-Prompts and Image-Prompts. *ACM Trans. Graph.*, 43(4), 2024. [3](#), [8](#)
- [59] Zhengxia Zou, Tianyang Shi, Shuang Qiu, Yi Yuan, and Zhenwei Shi. Stylized Neural Painting. In *2021 IEEE/CVF Conference on Computer Vision and Pattern Recognition (CVPR)*, pages 15684–15693, 2021. [3](#)